Time-Domain Analysis of Low-Speed Airfoil Flutter

K. D. Jones* and M. F. Platzer†

U.S. Naval Postgraduate School, Monterey, California 93943-5106

A time-domain aeroelastic analysis code is described for single airfoils and two-foil systems in incompressible, inviscid flow. Flow solutions are obtained using a time-stepping panel code, and airfoil motions are computed using a two-degree-of-freedom spring/mass model. The time-stepping aeroelastic code is evaluated through comparisons with several classical frequency-domain studies for single-degree-of-freedom pitching motion. Results show excellent agreement with past studies and provide a look into the evolution of the motion in time. Additionally, using a two-foil system, it is shown that flutter of a trailing airfoil can be controlled by proper oscillation and phasing of a leading airfoil. Three applications of the aeroelastic code are presented, including a feedback loop to actively stabilize flutter of a trailing airfoil, simulations of wake interference in rotary-wing flowfields, and simulations of flutter in ground effect.

Nomenclature

C_l	= lift coefficient per unit span
C_m	= pitching moment coefficient per unit span
c	= chord length
h	= bending displacement (positive downward)
h_g	= distance from ground
h_r	= wake spacing in rotary-wing flows
I_α	= moment of inertia about the elastic axis
K_h	= spring constant for plunging
K_α	= spring constant for pitching
k	= reduced frequency, $\omega c / V_\infty$
k_f	= reduced flutter frequency
k_h	= reduced natural plunging frequency, $\omega_h c / V_\infty$
k_α	= reduced natural pitching frequency, $\omega_\alpha c / V_\infty$
L	= lift per unit span
M	= pitching moment per unit span
m	= mass of the wing per unit span
m_r	= ω / Ω
q_{jk}	= source strength on panel j at t_k
r	= radius of rotary-wing blade section
S_α	= static moment, $x_\alpha m$
t	= time
V_α	= reduced velocity, $1/k_\alpha$
V_∞	= freestream velocity magnitude
X_{shift}	= horizontal offset of the control airfoil
x_p	= leading edge to elastic axis distance
x_α	= elastic axis to center of mass distance
Y_{shift}	= vertical offset of the control airfoil
α	= angle of attack
Γ_k	= circulation about the airfoil at t_k
γ_k	= vorticity per length on airfoil at t_k
γ_{w_k}	= vorticity per length on the wake panel at t_k
Δ_k	= length of wake panel at t_k
θ_k	= incidence of wake panel with respect to airfoil at t_k
λ	= wake wavelength, $2\pi/k$
ρ_∞	= freestream density
τ	= nondimensional time, $t V_\infty / c$
Ω	= rotary-wing rotational frequency
ω	= circular frequency
ω_h	= uncoupled natural bending frequency, $\sqrt{(K_h/m)}$
ω_α	= uncoupled natural torsional frequency, $\sqrt{(K_\alpha/I_\alpha)}$
$(\dot{\ })$	= differentiation with respect to t
$(\ )'$	= differentiation with respect to τ

Introduction

FOR many decades, scientists have been aware of the danger of structural failure because of aerodynamically driven oscillations. A classic example of this phenomenon occurred in 1940 when the Tacoma Narrows bridge, driven by the ambient wind, came apart after many hours of divergent resonation.[1] This behavior, called flutter, also occurs on aircraft wings and empennages, helicopter and propeller blades, and in turbomachines, such that applications for this research are plentiful. The study of these aerodynamically driven motions of flexible systems is referred to as aeroelasticity.

Most flutter codes used in the aerospace industry are based on linearized oscillatory aerodynamic theory as input into the flutter equations, solving the flutter problem in the frequency domain rather than in the time domain. However, many modern computational fluid dynamics codes employ a time-marching approach that suggests that the use of such codes for the prediction of airfoil/blade flutter and dynamic response may become a practical approach in the near future.

The current method utilizes such a time-stepping approach with an unsteady panel method to describe the inviscid, incompressible flowfield and with a two-degree-of-freedom spring/mass system to model the bending/torsion flutter. The algorithms used in the code are outlined in the following sections as well as the applications for active flutter suppression, wake-induced flutter in rotary-wing flowfields, and flutter in ground effect. Some of this work has been presented earlier in Ref. 2.

Approach

Aeroelasticity is a multidisciplinary subject combining aerodynamics and structural dynamics. The methods used for each of these fields are outlined in this section. Additionally, the methods used for the feedback control loop are discussed, and the applications to active flutter control, the simulation of wake interference in rotary-wing flowfields, and the simulation of flutter in ground effect are described.

Aerodynamics

Consider incompressible, inviscid flow over two airfoils of arbitrary geometry that may execute an arbitrary motion relative to each other. The basic governing equation for this problem is the Laplace equation.

In the past, a number of investigators have solved the steady flow problem using source and vortex paneling, the most prominent ones being Hess and Smith.[3] A few authors have extended this approach to the case of unsteady motion of single airfoils, notably Basu and Hancock[4] and Kim and Mook.[5] Teng[6] developed a computer code for the numerical solution of unsteady, inviscid, incompressible flow

over an airfoil. Teng's work was extended by Platzer et al.[7] to investigate interference effects with multiple airfoils. Each airfoil surface is approximated by a large number of surface elements, and a uniform source distribution and vorticity distribution are placed on each element. The source strength varies from element to element, whereas the vortex strength is the same for all elements. The singularity strengths are determined from the flow tangency condition on both airfoil surfaces and the Kutta condition at each trailing edge.

The unsteady flow problem differs from the steady flow problem in that the continuous shedding of vorticity into each foil's trailing wake needs to be included in the computation. According to the vorticity conservation theorem, any change in circulation around an airfoil must be matched by an equal and opposite vortex shed from the foil's trailing edge. The presence of the countervortices provides the flow with a kind of memory in that the flow at a particular time is affected by the bound circulation of the past. It is this influence that distinguishes the numerical technique required for the unsteady flow solution from the simpler steady flow problem of solving N linear equations in N unknowns.

The present approach follows closely the original panel method of Hess and Smith,[3] whereas with regard to the modeling of the wake it adopts the procedure advocated by Basu and Hancock.[4] Uniform source and vorticity distributions are placed on each panel at time t. The wake consists of a single vorticity panel attached as an additional element on each airfoil through which discrete vortices are shed into the respective wake and convected downstream with the fluid. A uniform vorticity distribution is placed on the wake panel of each airfoil. This panel is further characterized by its length Δ_k and its inclination with respect to the local frame of reference θ_k. After each time step, the vorticity of the wake panel is concentrated into a single point vortex and convected downstream. Simultaneously, a new wake panel is formed.

The flow tangency conditions are satisfied at the exterior midpoints (control points) of each panel. The Kutta condition postulates that the pressure on the upper and lower surface at the trailing edge of each foil be equal. The wake panels are formed with a length and inclination to the respective local frames of reference that satisfy the Helmholtz theorem

$$\Delta_k(\gamma_w)_k + \Gamma_k = \Gamma_{k-1} \qquad (1)$$

This unsteady flow model introduces an additional boundary condition, the conservation of vorticity. However, the introduction of the wake creates three additional unknowns for each airfoil: the vorticity of the wake panel, its length, and its inclination. Therefore, two additional conditions are required for each airfoil to solve the system. The approach suggested by Basu and Hancock[4] is extended to the two-foil case.

1) Each wake panel is oriented in the direction of the local resultant velocity at the panel midpoint.

2) The length of each wake panel is proportional to the magnitude of the local resultant velocity at the panel midpoint and the size of the time step.

The essential elements of this scheme are summarized in Fig. 1. Implementation of this approach requires an iterative scheme, since the velocity direction and magnitude at the panel midpoints are not initially known.
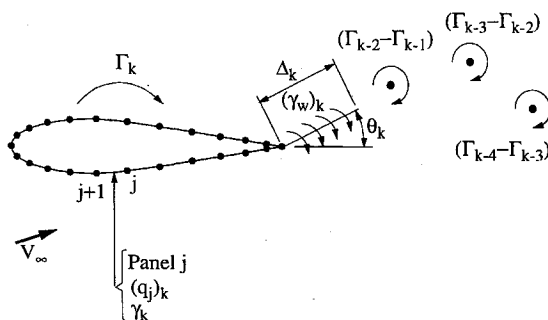
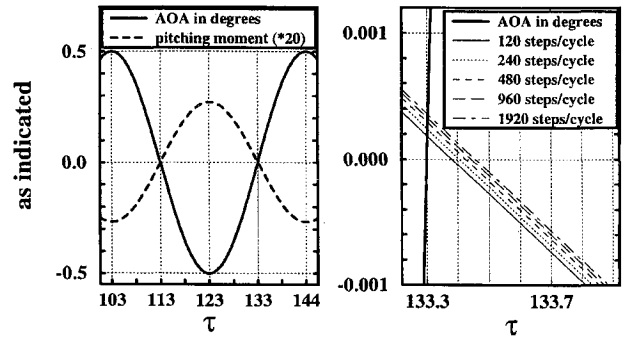

Fig. 1   Schematic of unsteady wake representation.

Fig. 2   Panel code step-size dependency.

In classical aeroelastic studies the wake is confined to the plane that the airfoil lies in with a sinusoidal vorticity distribution thereby maintaining linearity in the solution procedure. Here the wake is modeled by a finite stream of discrete vortices, with a new vortex released by each airfoil at each time step, and the vortices convect through the flow, influencing and being influenced by the airfoils and all of the other vortices. Thus, the iterative wake panel determination and the discrete vortex wake modeling are nonlinear effects and result in a new class of nonlinear solutions.

Details of the single and two airfoil codes are given in Refs. 6 and 8, respectively. A thorough evaluation of the accuracy of the panel code was performed by Riester[9] by comparing the computed lift and moment coefficients for both pitch and plunge motions with those of Theodorsen and Garrick.[10]

Past studies, as well as the present, have noted a small step-size dependency of the potential flow code, resulting in slight phase errors in the predicted unsteady lift and moment values. Results are shown in Fig. 2 for a NACA 0012 airfoil pitching sinusoidally about its leading edge with a reduced frequency of 0.1532 and an amplitude of ±0.5 deg. The sinusoidal motion and the resulting sinusoidal moment coefficient are shown in the left graph with a detailed view shown in the right graph. Flutter occurs when C_m is 180 deg out of phase from the pitch angle α, and it can be seen that as the number of steps/cycle is varied, the predicted phase and, hence, the predicted flutter frequency change. The dotted, vertical grid lines on the right graph correspond to 1-deg increments in phase. There is slightly less than a 1-deg phase change between the cases with 120 and 1920 steps/cycle. This phase error is not large but will affect the predicted flutter boundaries for both frequency-domain and time-domain studies. The step size may not be reduced indefinitely. First, as the step size is reduced, the vorticity of the discrete wake vortices decreases and eventually cannot be resolved. Second, the computational time for a simulation increases as roughly the square of the number of total steps, such that the panel code becomes more expensive than Euler or Navier–Stokes simulations if more than a few thousand time steps are used. The cases with 960 and 1920 steps/cycle required double precision accuracy to resolve the wake vorticity, and the latter case required about eight times the CPU time needed for a comparable Euler simulation. However, typical panel code simulations with around 120 steps/cycle require only about 5% of the CPU time needed for an Euler solution; therefore, it is a good choice for developing and evaluating the time-domain aeroelastic approach.

The incompressible panel code is limited to low-speed calculations. For steady solutions the approximation of incompressibility is generally considered accurate to a Mach number of around 0.3, but in unsteady flows the Mach number dependence becomes much stronger because of the waves generated by the airfoil oscillations.

The panel code does permit wake interference studies including wake impingement on the trailing airfoil if a sufficiently small time step is used. Results are shown for a NACA 0012 airfoil plunging with a reduced frequency of 1.5, an amplitude of ±0.2c, and with a second, stationary NACA 0012 airfoil a chord length downstream. The simulation has 240 steps/cycle, and individual wake vortices are plotted for a sequence of time steps in Fig. 3. The circles and squares correspond to discrete wake vortices from the leading and trailing airfoils, respectively. Clearly, the wake from the leading airfoil is
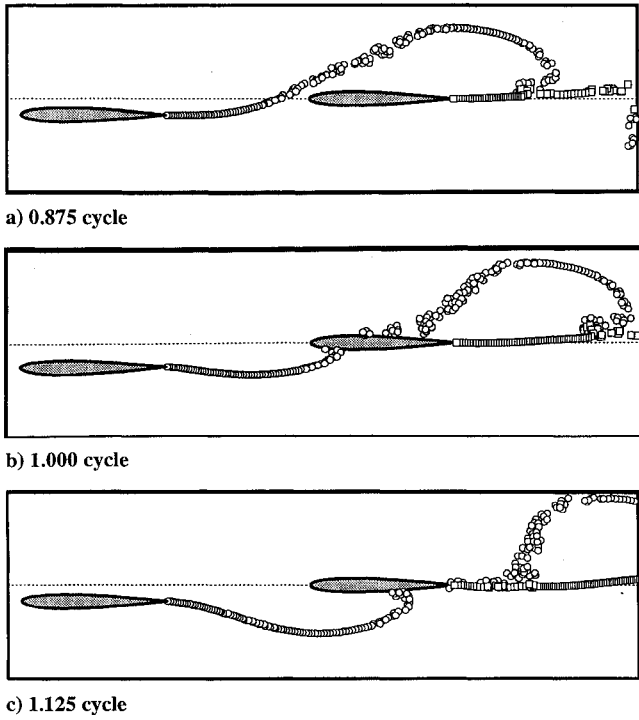
a) 0.875 cycle

b) 1.000 cycle

c) 1.125 cycle

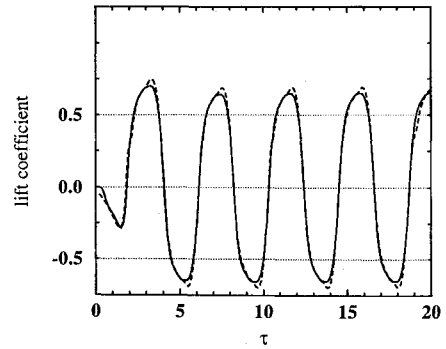**Fig. 3   Wake impinging a stationary trailing airfoil.**

Fig. 4   Lift on the trailing airfoil: ——, Navier–Stokes (Ref. 11) and ----, panel code (smoothed).

Fig. 5   Schematic of the aeroelastic two-foil system.

impinging the trailing airfoil. The wake is split and the discrete vortices are deflected around the upper and lower surfaces of the trailing airfoil. The computed lift on the trailing airfoil is plotted in Fig. 4 with a comparison to the Navier–Stokes simulation of Tuncer and Platzer.[11] Note that the plotted lift values from the panel code are smoothed using localized averaging. High-frequency fluctuations in the lift result from numerical resolution errors of the small distances between the wake vortices and the trailing airfoil control points. The smoothed results compare well with the Navier–Stokes solution, but the high-frequency fluctuations make aeroelastic computations difficult; hence, the present work is limited to wake interference where the interfering wake does not directly contact the free airfoil.

Structural Dynamics

Structural modeling is facilitated using a two-degree-of-freedom spring/mass system (Fig. 5) to simulate the bending and twisting of a wing. The equations governing this motion are

$$m\ddot{h} + S_\alpha\ddot{\alpha} + m\omega_h^2 h = -L \tag{2}$$

and

$$S_\alpha\ddot{h} + I_\alpha\ddot{\alpha} + I_\alpha\omega_\alpha^2\alpha = M \tag{3}$$

Note that Eqs. (2) and (3) assume that α is small, since $\cos\alpha$ is replaced with 1.0 in the coupling term.

Nondimensionalizing the system using reference values of length $= c$, velocity $= V_\infty$, time $= c/V_\infty$, and mass $= c^2\pi\rho_\infty/4$, and rewriting the system in matrix notation, one obtains

$$[M]\{X\}'' + [k]\{X\} = \{F\} \tag{4}$$

where

$$[M] = \begin{bmatrix} m & S_\alpha \\ S_\alpha & I_\alpha \end{bmatrix}, \qquad [k] = \begin{bmatrix} m\omega_h^2 & 0 \\ 0 & I_\alpha\omega_\alpha^2 \end{bmatrix}$$

$$\{X\} = \begin{Bmatrix} h \\ \alpha \end{Bmatrix}, \qquad \{F\} = \frac{2}{\pi}\begin{Bmatrix} -C_l \\ C_m \end{Bmatrix}$$

Equation (4) is a system of two coupled, second-order, nonlinear, differential equations, coupled through the terms containing S_α and the dependence of C_l and C_m on h and α, and nonlinear through

the dependence of C_l and C_m on the nonlinear wake model. Single-degree-of-freedom simulations are performed by setting $S_\alpha = 0$ and either $m = \infty$ and $\omega_h = 0$ or $I_\alpha = \infty$ and $\omega_\alpha = 0$ for pitching-only or plunging-only motions, respectively.

Equation (4) is advanced in time by inverting the system, yielding

$$\{X\}'' = [M]^{-1}\{F\} - [M]^{-1}[k]\{X\} \tag{5}$$

then rewriting the result as a system of two coupled, first-order equations

$$\{X\}' = \{Y\}$$
$$\{Y\}' = [M]^{-1}\{F\} - [M]^{-1}[k]\{X\} \tag{6}$$

and, finally, integration is performed using either a second-order modified Euler scheme or a fourth-order Runge–Kutta scheme. Note that the iterative modified Euler scheme reduces to a second-order Runge–Kutta scheme if just two iterations are used.

The two-degree-of-freedom spring/mass integration procedure was validated by setting $C_l = C_m = 0$ (simulating an undamped system) and computing the total energy (kinetic and potential) of the system at each time step. With as few as 30 steps per cycle the fourth-order scheme computed less than a 0.005% loss in total energy per cycle for coupled or uncoupled motions.

Feedback Control Loop

A certain amount of feedback is inherent in a single-foil system through the aerodynamic modeling of the wake and its influence on the airfoil. The influence of this feedback is necessarily small, since the wake rapidly convects downstream. However, in a two-foil system the wake of an upstream airfoil may pass very near or come into contact with and may have a substantial influence on the aeroelastic behavior of a downstream foil. With this in mind, it is desirable to move an upstream control airfoil in a manner that suppresses flutter in a downstream free airfoil.

A system diagram representing the two-foil system is shown in Fig. 6a, where $\alpha_{1_i}(t)$ is an initial pitch disturbance of the free airfoil and $\alpha_2(t)$ defines the motion of the control airfoil. The aerodynamic model takes the position of both foils as input and provides lifts
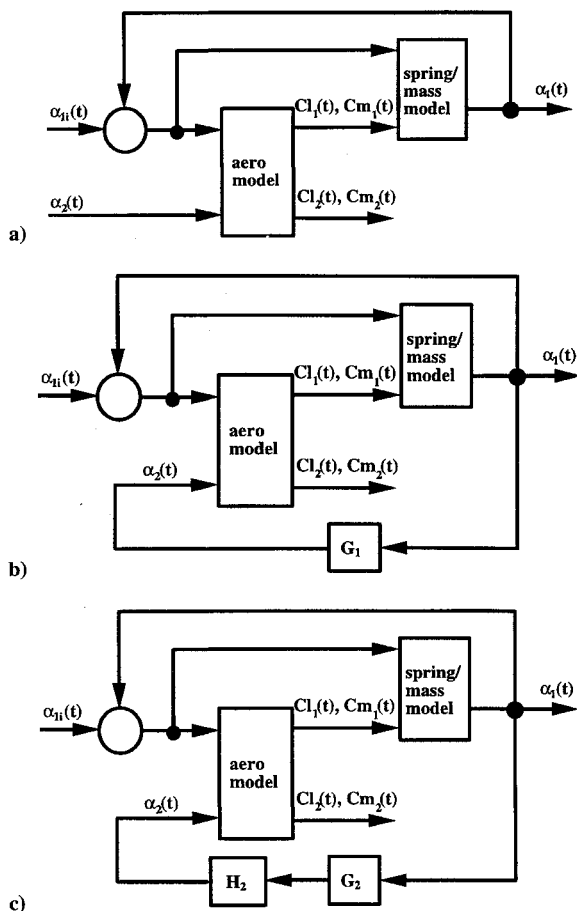
Fig. 6 System diagrams of a) basic two-foil system, b) first feedback loop, and c) second feedback loop.

a)

b)

Fig. 7 Rotary-wing wake representations of a) Loewy[12] and b) present.

Ground level

Image airfoil and image wake

Fig. 8 Schematic of ground effect simulations.

and moments of both foils as output. Note that the aerodynamic model also includes memory in the form of the convecting wake structures, and the wake provides an additional form of feedback. The free airfoil has a spring/mass model that accepts the lift and moment as well as the airfoil position as input and results in a new airfoil position that is then fed back into the loop.

Two methods are provided for controlling the motion of one airfoil based on the free aeroelastic motion of another. The first provides a simple feedback loop, as shown in Fig. 6b, with only gain control (G_1 = const). Note that phase control of the feedback signal is available through the geometric placement of the control airfoil, since the time necessary for the wake to convect downstream to the position of the free airfoil results in a signal phase delay.

The second feedback loop, shown in Fig. 6c, provides a more sophisticated gain control and an additional phase control. Here the gain is varied to maintain a roughly constant pitch amplitude of the control airfoil until the pitch amplitude of the free airfoil drops below a threshold value, at which time the gain switches to a constant value. These feedback loop capabilities are used in the three applications described next.

Rotary-Wing Flows

Simulations of wake interference in rotary-wing flowfields are performed in a two-dimensional, strip-theory fashion similar to the approach of Loewy.[12] Loewy approximated the helical wake structure beneath a hovering helicopter at a given radial station by a two-dimensional flow with a single blade section and an infinite series of wakes beneath it (Fig. 7a). The wake separation h_r is a function of the inflow velocity, and the phasing is determined by the ratio of the pitching frequency to the rotational frequency ω/Ω. The interfering wakes are assumed to extend to $\pm\infty$.

In the present approach only a single interfering wake of finite length is considered, and this is facilitated by placing a second blade upstream a distance $2\pi r$ (the circumferential length for a given radius) and below the first blade the distance h_r (Fig. 7b). The
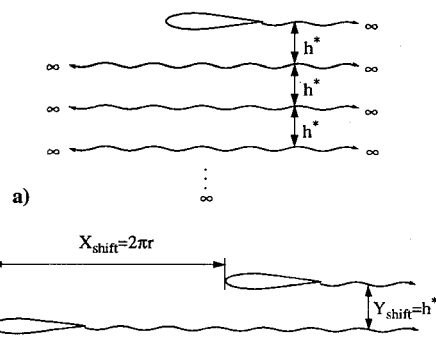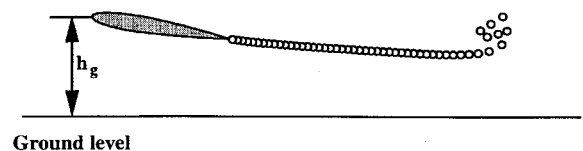
reduced pitching frequency is determined directly from the specified frequency ratio m_r.

The interfering wake is intended to represent the wake from the previous blade or, for a one-bladed system, from the reference blade after one rotation. To model this the upstream blade is moved exactly as the reference blade, such that the vortex street created by the upstream blade is a clone of the vortex street created by the reference blade. This approach incorporates the first feedback option using an amplitude scale factor of 1.

Flutter in Ground Effect

The potential flow about a body in the presence of a wall is computed by creating a mirror image of the body within the wall. Therefore, the flow about an airfoil in ground effect is simulated by placing an image airfoil underground (Fig. 8).

To model the aeroelastic behavior of an airfoil in ground effect, the fictitious second airfoil is moved in a mirror-image fashion, employing the first feedback option with an amplitude scale factor of -1.

Active Flutter Suppression

As shall be seen, the suppression of flutter through fixed sinusoidal motions of a control airfoil is transitory at best, since the frequency and phase of the free airfoil are not fixed in time. To stabilize the free airfoil for all time, an active control loop is required.

The first feedback option will stabilize the free airfoil but, since the stabilizing effect of the interfering wake is proportional to the magnitude of the wake vorticity, which is proportional to the oscillation amplitude of the control airfoil, the rate at which the amplitude is dampened diminishes as $1/t$.

The second feedback approach stabilizes the free airfoil much more quickly. In fact, as will be shown, this approach reduces the oscillation amplitude of the free airfoil linearly in time. When the motion becomes sufficiently damped, the algorithm switches to the first feedback approach.

Results

The following subsections present results of single- and two-airfoil systems undergoing single-degree-of-freedom pitching motions. Results are presented demonstrating the accuracy of the time-stepping approach through comparisons with theory and other numerical studies. Additionally, results are presented for the three applications illustrating the utility of the time-stepping aeroelastic code.

Single Airfoil

Results for a single airfoil undergoing pitching motions are compared with the classical works of Theodorsen and Garrick[10] and of Smilg[13] and the more contemporary work of Turner.[14] Theodorsen and Garrick considered the pitching motion of a flat plate with arbitrary k_α and I_α about a specified elastic axis x_p. They showed that the frequency at which flutter occurred, k_f, was independent of I_α, and for $x_p = 0$, $k_f \approx 0.08$.

In the present method the airfoil is released with a small angle-of-attack displacement at $\tau = 0$, and the resulting motion is computed as a function of time. Sample time histories of α are given in Fig. 9 at a stable, a neutral, and an unstable frequency for a NACA 0007 airfoil pivoting about its leading edge ($x_p = 0$) with $I_\alpha = 150$.

The resultant pitching frequency predicted by the present approach is compared with the flat-plate results in Fig. 10 for a spectrum of airfoil thicknesses and I_α, all with $x_p = 0$. Each cluster of three curves corresponds to the value of I_α indicated in the legend, with the lower, middle, and upper line of each threesome corresponding to NACA 0001, NACA 0007, and NACA 0012 airfoils, respectively. The symbols $\bigcirc$, $\square$, and $\Diamond$ are located at the predicted flutter frequencies for the different airfoils and I_α values (i.e., the frequency where the oscillation amplitude remains constant). Note that for each of the NACA airfoils k_f is constant with respect to I_α, and even though the frequency response does not change much with thickness, the flutter frequency changes significantly. As I_α increases, the effect of thickness becomes less apparent in the frequency response, and the curves approach the theoretical undamped response for $I_\alpha = \infty$.

According to Smilg,[13] a flat plate will not flutter for I_α less than about 143. This is indicated by the frequency response curves shown in Fig. 10. For I_α lower than about 150 the response curves do not intersect the line $k_f = 0.08$.

The method employed by Turner[14] used the current panel code, pitching the airfoil sinusoidally. A sinusoid was fit to the resulting C_m curve, and stability was determined by the sign of the out-of-phase portion. For a NACA 0007 airfoil Turner predicted
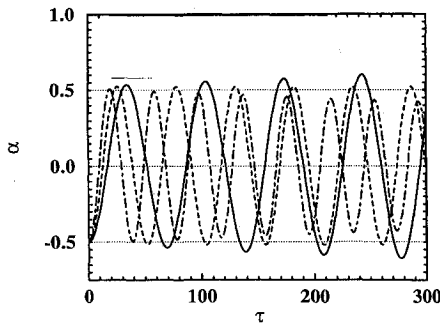
Fig. 9   Time history of α as a function of k_α: ——, $k_\alpha = 0.04$ and $k = 0.0905$; ---, $k_\alpha = 0.09$ and $k_f = 0.1205$; and ----, $k_\alpha = 0.15$ and $k = 0.1606$.
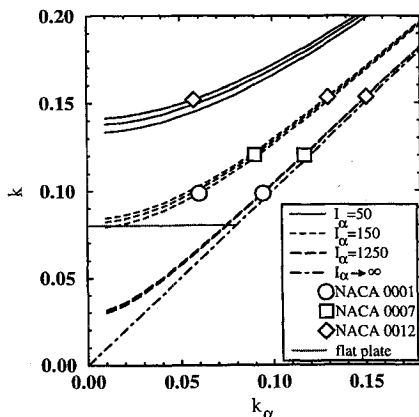
Fig. 10   Resultant pitching frequency and flutter boundaries.

$k_f \approx 0.115$, whereas the present method predicts $k_f \approx 0.120$. This much variation can be accounted for by variations in step size.

Two Airfoils

Airfoil/wake interference simulations with two airfoils are compared with the frequency-domain work of Turner. For these cases the leading or control airfoil is pitched sinusoidally about its leading edge with pitch amplitude $\alpha = \pm 0.5$ deg and with chord lengths of 1, $\frac{1}{2}$, $\frac{1}{4}$, and $\frac{1}{10}$. The trailing airfoil starts at $\alpha = -0.5$ deg and is released in phase with the control airfoil with $x_p = 0$, $I_\alpha = 150$, and $k_\alpha = 0.0585$. In the absence of the leading airfoil, these conditions yield an unbounded pitching motion with $k = 0.1$. The control airfoil is placed two chord lengths below the reference airfoil ($Y_{\text{shift}} = -2$) and a variable distance upstream, with X_{shift} varied between 0 and -63 (in nondimensional space $\lambda \approx 63$) providing a full spectrum of wake phase angles.

Values of X_{shift} resulting in flutter suppression or amplification agree well with Turner. Sample plots are shown in Fig. 11 for cases that are initially stable, neutral, and unstable. Flutter is suppressed at $X_{\text{shift}} = -14$ ($\approx -\lambda/4$), and flutter is induced at $X_{\text{shift}} = -44$ ($\approx -3\lambda/4$).

Of particular interest is the evolution of the free-airfoil motion in time, a facet of the problem not captured by the frequency-domain methods. The motion with $X_{\text{shift}} = -14$, although initially stable, changes phase by 180 deg once the pitch magnitude is small, and then the motion becomes unstable. This phase/magnitude relationship is illustrated in Fig. 12. The phase of the case that is initially unstable remains unchanged for all time, but the phase for the case that is initially neutral begins to drift toward an unstable mode immediately. This tendency for the phase to drift to unstable modes was previously noted in Ref. 15.

Rotary-Wing Flows

The effect of wake interference in rotary-wing flowfields is qualitatively compared with the frequency-domain work of Loewy.[12] The effect of wake interference from the preceding blade on the pitch stability of the reference blade is shown for pitch oscillations about the leading edge. The blade has a NACA 0007 profile, $I_\alpha = 375$, and $Y_{\text{shift}} = -h_r = -2.5$. The present time-domain approach provides the decay or growth of the pitch oscillation; therefore, the time rate of change of pitching amplitude is a convenient measure of the stability or instability of the pitch oscillation and is plotted on the ordinate
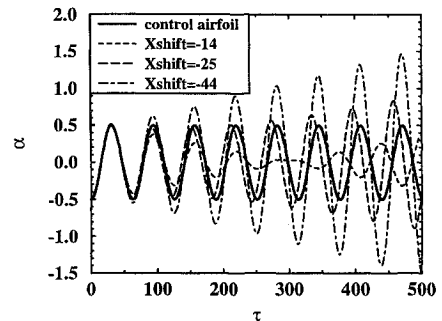
Fig. 11   Time history of α as a function of X_{shift}.
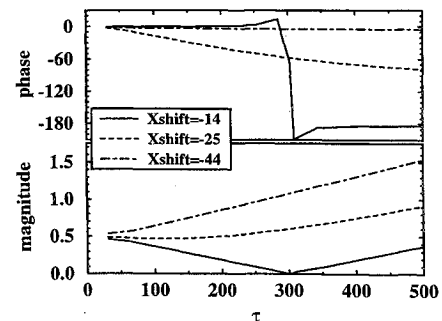
Fig. 12   Phase/magnitude relationship.

of Fig. 13 as a function of Loewy's frequency ratio m_r on the abscissa. For conventional cyclic inputs, $m_r = 1$ since blade pitching is mechanically coupled to blade rotation via the swashplate, but for higher harmonic control and multibladed rotor systems, m_r will typically be noninteger. Since $k = m_r/r$, a variation of m_r implies a variation of k for a given radial station r and thus a relative shifting of the phase between the impinging wake vorticity and the reference blade motion. In Fig. 13, $r = 8$, resulting in $X_{shift} \approx 50$.

In the absence of the interfering wake, a single airfoil with the stated characteristics becomes unstable at reduced frequencies below about 0.12, as shown by the dashed line in Fig. 13. Although the single blade is stable for $k > 0.12$ ($m_r > 0.96$), the inclusion of wake interference from the preceding blade produces a second region of instability for $1.52 \le m_r \le 1.84$. The stabilizing/destabilizing effect of the impinging wake is essentially sinusoidal with period m_r, promoting stability through half the cycle and instability for the other half. The magnitude of the interference effect diminishes with increasing m_r, such that for higher values of m_r no instability occurs. Figure 15 of Ref. 11 shows a similar phenomenon.

Flutter in Ground Effect

Simulations are presented for a NACA 0007 airfoil, pitching about the leading edge, with $I_\alpha = 150$. Far from the ground it was found that an airfoil with these characteristics becomes unstable for $k < 0.12$. Here a naturally unstable frequency is used ($k = 0.1$) and the time rate of change of the pitching amplitude is plotted as a function of h_g/c in Fig. 14. Note that the motion is stable for very low level flight, but flutter is induced for $h_g/c > 3$. The airfoil is most unstable at $h_g/c \approx 7$, and this agrees well with Ref. 14.

Active Control Loop

The short-lived success of flutter suppression demonstrated in Fig. 11 suggests the use of an active control loop for determining appropriate motions of a control airfoil. Using the second feedback loop previously discussed with the same airfoil configuration as that used in Fig. 11, and with the control airfoil located at $-\lambda/4$, the free-airfoil motion is rapidly damped. Results are shown for a control airfoil of chord length 1 (Fig. 15) and 1/16 (Fig. 16).

Airfoil separations other than $-\lambda/4$ are possible if an appropriate signal phase delay is given; however, because of the increased time
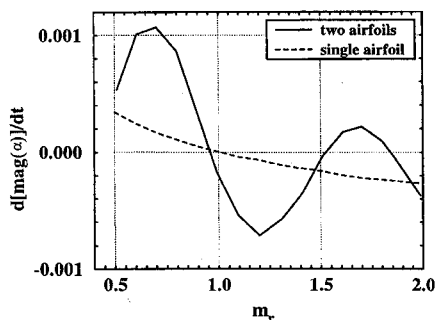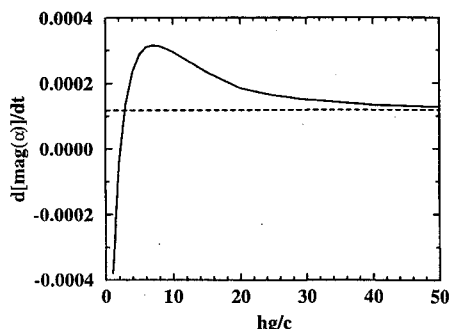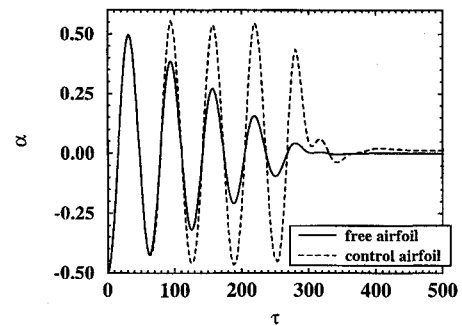

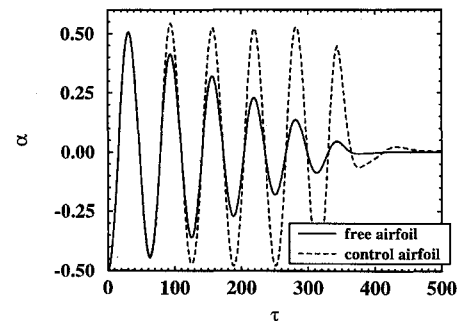**Fig. 15 Flutter suppression through active control (scale = 1).**

Fig. 16 Flutter suppression through active control (scale = 1/16).

delay required for the wake vorticity to convect downstream to the free airfoil, complete damping becomes difficult.

Conclusions

A time-stepping flutter analysis code was introduced, combining an unsteady, two-foil panel code with a two-degree-of-freedom spring/mass structural dynamic model for simulating inviscid, incompressible flows. The accuracy and limitations of the approach were demonstrated through comparisons with past frequency-domain studies for single-degree-of-freedom pitching motions.

Computed results agreed well with the frequency-domain results. The time-stepping approach provided the additional capability to analyze the evolution of the motion in time. Qualitatively, trends in the resultant pitching frequency due to sectional thickness and moment of inertia were clearly correct, and quantitative agreement was within the expected bounds afforded by the panel method.

Feedback loop algorithms were developed, and the included results demonstrated their success in simulating wake interference in rotary-wing flows, flutter in ground effect, and actively suppressing flutter.

Wake interference in rotary wing flows was modeled by placing a second airfoil an appropriate distance upstream to simulate the interfering wake from the previous blade. The computed stability boundaries agreed well with past frequency domain studies.

Flutter in ground effect was simulated by placing an image airfoil within the ground, moving in a mirror-image fashion. Presented results demonstrated the stabilizing effect of low-level flight and suggest that vehicles designed to fly in ground effect do so at an altitude of less than three chord lengths. For the conditions tested, it was shown that flight near a ground plane at higher altitudes promotes instability. A more extensive study of the conditions promoting stability and instability is recommended in the future.

Active control simulations indicated that the controlling airfoil remains effective even with greatly reduced chord lengths, but that effectiveness was lost as the distance between the foils increased. This suggests that a closely placed canard or leading-edge flap may be sufficient for controlling flutter.

The time-domain approach presented here is quite robust and efficient. Typical single airfoil simulations run on a workstation in a few minutes. The active control loop, ground effect, and rotary-wing simulations demonstrate just a few of the many applications of the time-domain approach.

Fig. 13 Pitch stability in rotary-wing flows.

Fig. 14 Pitch stability in ground effect: ——, in ground effect and ----, out of ground effect.

Acknowledgment

References

[1] Sisto, F., "Introduction and Overview," *AGARD Manual on Aeroelasticity in Axial-Flow Turbomachines: Vol. 1, Unsteady Turbomachinery Aerodynamics*, edited by M. F. Platzer and F. O. Carta, AGARDograph No. 298, 1987, pp. 1-1, 1-8.

[2] Jones, K. D., and Platzer, M. F., "Time-Domain Aeroelastic Analysis of a Two Airfoil System with Application to Unsteady Rotary Wing Flowfields," AIAA Paper 95-0337, Jan. 1995.

[3] Hess, J. L., and Smith, A. M. O., "Calculation of Potential Flow About Arbitrary Bodies," *Progress in Aeronautical Sciences*, Vol. 8, Pergamon, Oxford, England, UK, 1966, pp. 1–138.

[4] Basu, B. C., and Hancock, G. J., "The Unsteady Motion of a Two-Dimensional Aerofoil in Incompressible Inviscid Flow," *Journal of Fluid Mechanics*, Vol. 87, Pt. 1, 1978, pp. 159–168.

[5] Kim, M. J., and Mook, D. T., "Application of Continuous Vorticity Panels to General Unsteady Incompressible Two-Dimensional Lifting Flows," *Journal of Aircraft*, Vol. 23, No. 6, 1986, pp. 464–471.

[6] Teng, N. H., "The Development of a Computer Code for the Numerical Solution of Unsteady, Inviscid and Incompressible Flow over an Airfoil," M.S. Thesis, Dept. of Aeronautics and Astronautics, U.S. Naval Postgraduate School, Monterey, CA, June 1987.

[7] Platzer, M. F., Neace, K. S., and Pang, C. K., "Aerodynamic Analysis of Flapping Wing Propulsion," AIAA Paper 93-0484, Jan. 1993.

[8] Pang, C. K., "A Computer Code for Unsteady Incompressible Flow Past Two Airfoils," Aeronautical Engineer's Thesis, Dept. of Aeronautics and Astronautics, U.S. Naval Postgraduate School, Monterey, CA, Sept. 1988.

[9] Riester, P. J., "A Computational and Experimental Investigation of Incompressible Oscillatory Airfoil Flow and Flutter Problems," M.S. Thesis, Dept. of Aeronautics and Astronautics, U.S. Naval Postgraduate School, Monterey, CA, June 1993.

[10] Theodorsen, T., and Garrick, I. E., "Mechanism of Flutter," NACA TR-685, 1940.

[11] Tuncer, I. H., and Platzer, M. F., "Analysis of Unsteady Airfoil Interference Effects Using a Zonal Navier–Stokes Solver," AIAA Paper 95-0307, Jan. 1995.

[12] Loewy, R. G., "A Two-Dimensional Approximation to the Unsteady Aerodynamics of Rotary Wings," *Journal of the Aeronautical Sciences*, Vol. 24, No. 2, 1957, pp. 81–106.

[13] Smilg, B., "The Instability of Pitching Oscillations of an Airfoil in Subsonic Incompressible Potential Flow," *Journal of the Aeronautical Sciences*, Vol. 16, No. 11, 1949, pp. 691–696.

[14] Turner, M., "A Computational Investigation of Wake-Induced Airfoil Flutter in Incompressible Flow and Active Flutter Control," M.S. Thesis, Dept. of Aeronautics and Astronautics, U.S. Naval Postgraduate School, Monterey, CA, March 1994.

[15] Bakhle, M. A., Reddy, T. S. R., and Keith, T. G., Jr., "Time Domain Flutter Analysis of Cascades Using a Full-Potential Solver," *AIAA Journal*, Vol. 30, No. 1, 1992, pp. 163–170.